Local carrier recombination and associated dynamics in *m*-plane InGaN/GaN quantum wells probed by picosecond cathodoluminescence

Tongtong Zhu,[1,a)] David Gachet,[2] Fengzai Tang,[1] Wai Yuen Fu,[3] Fabrice Oehler,[1,b)] Menno J. Kappers,[1] Phil Dawson,[4] Colin J. Humphreys,[1] and Rachel A. Oliver[1]
[1]*Department of Materials Science and Metallurgy, University of Cambridge, 27 Charles Babbage Road, Cambridge CB3 0FS, United Kingdom*
[2]*Attolight AG, EPFL Innovation Park, Building D, CH-1015 Lausanne, Switzerland*
[3]*Department of Electrical and Electronic Engineering, The University of Hong Kong, Pokfulam Road, Hong Kong*
[4]*School of Physics and Astronomy, Photon Science Institute, University of Manchester, Manchester M13 9PL, United Kingdom*

(Received 17 August 2016; accepted 21 November 2016; published online 5 December 2016)

We report on spatially resolved and time-resolved cathodoluminescence (CL) studies of the recombination mechanisms of InGaN/GaN quantum wells (QWs) grown by metal-organic vapour phase epitaxy on bulk *m*-plane Ammono GaN substrates. As a result of the 2° miscut of the GaN substrate, the sample surface exhibits step bunches, where semi-polar QWs with a higher indium concentration than the planar *m*-plane QWs form during the QW growth. Spatially resolved time-integrated CL maps under both continuous and pulsed excitation show a broad emission band originating from the *m*-plane QWs and a distinct low energy emission originating from the semi-polar QWs at the step bunches. High resolution time-resolved CL maps reveal that when the *m*-QWs are excited well away from the step bunches the emission from the *m*-plane QWs decays with a time constant of 350 ps, whereas the emission originating semi-polar QWs decays with a longer time constant of 489 ps. The time constant of the decay from the semi-polar QWs is longer due to the separation of the carrier wavefunctions caused by the electric field across the semi-polar QWs. *Published by AIP Publishing.* [http://dx.doi.org/10.1063/1.4971366]

The use of non-polar InGaN/GaN quantum wells (QWs) in light emitting diodes (LEDs) offers the possibility of improved device performance compared with LEDs that incorporate polar QWs. This is because of the elimination of the polarization and piezoelectric fields across the QWs which leads to an increased overlap between the electron-hole wave functions, and hence shorter radiative lifetimes.[1,2] Thus the internal quantum efficiency of non-polar LEDs should be higher than their polar counter parts, as the radiative channel is better able to compete with any non-radiative pathways. Also because of the absence of a quantum confined Stark effect, non-polar LEDs have been shown to exhibit a reduced blue-shift in emission wavelength with increasing current density.[3]

Development of high performance non-polar LEDs has benefitted from the improved availability of free-standing/bulk GaN substrates.[4,5] Also the use of low-defect density GaN substrates has enabled the growth of InGaN QWs where the spectral quality of the emission is such that we can gain improved understanding of the fundamental physics of the QW emission, which in turn may ultimately lead to better device performance. There have been significant steps forward in the understanding of the fundamental recombination processes, at low temperatures, with the dominant recombination believed to involve localised excitons.[6–8] One particular characteristic of this recombination mechanism is the large photoluminescence (PL) line width, typically 100–200 meV, which is governed by the effects of localisation of holes at different sites in the wells. However, multiple emission peaks have also been observed from *m*-plane InGaN QWs and attributed to localised and extended states.[7] In addition, the metal-organic vapor phase epitaxy (MOVPE) regrowth of GaN layers on bulk GaN substrates, either obtained from vapor phase epitaxy[9] or ammonothermal[10] methods, is known to strongly depend on the substrate features. Structural quality and misorientation of the initial GaN substrate surface have been shown to strongly impact the subsequent homoepitaxial growth of GaN by forming pyramidal hillocks[11] or inclined facets,[6] which significantly affect the local indium incorporation and thus the emission line width from non-polar InGaN/GaN QWs.

In this paper, we report on detailed microstructural and optical characterization of *m*-plane InGaN/GaN multiple quantum wells (MQWs) grown on bulk Ammono GaN substrates. We specifically focus on the low energy emission component which originates from semi-polar QWs formed at the step bunches due to the 2° GaN substrate miscut towards [000-1]. Spatially resolved and time-resolved cathodoluminescence (CL) measurements have allowed us to directly probe the local carrier dynamics by not only showing that the low energy emission tails in the spectra are indeed from semi-polar QWs formed across step bunches, but are also providing insights into the carrier recombination processes at different local positions.

[a)]Author to whom correspondence should be addressed. Electronic mail: tz234@cam.ac.uk
[b)]Current address: C2N – Centre for Nanoscience and Nanotechnology, Site Marcoussis, Route de Nozay, 91460 Marcoussis, France.

The sample studied was grown by MOVPE in a 6×2 in. Thomas Swan close-coupled showerhead reactor on bulk Ammono *m*-plane GaN substrates. The substrates had a miscut of $2 \pm 0.2°$ towards [000-1], a nominal threading dislocation density of less than $5 \times 10^4\,cm^{-2}$ and a negligible density of stacking faults.[10] Trimethylgallium, trimethylindium, and ammonia were used as precursors, and hydrogen and nitrogen were used as carrier gases for GaN and InGaN/GaN QW growth, respectively. An unintentionally doped GaN buffer layer of thickness $\sim 2\,\mu m$ was grown at a temperature of 1050 °C and a pressure of 100 Torr, followed by the growth of 5-periods of InGaN/GaN QWs using a quasi-two temperature method.[12] Each QW was grown and then capped by ~1 nm of GaN grown at 735 °C, and the barrier growth continued as the temperature was ramped to 855 °C in 90 s, at which temperature the barrier growth was completed. The thicknesses of the InGaN QWs and GaN barriers were measured at 2.6 ± 0.2 nm, and 5.7 ± 0.2 nm, respectively, and the indium content of the InGaN QWs at 21%.[13] The surface morphology was analysed by atomic force microscopy (AFM) using a Veeco Dimension 3100 in TappingMode™. Cross-sectional TEM specimens were prepared by a DualBeam™ focused ion beam (FIB) microscope (FEI Helios) using an *in-situ* lift-out method. High resolution high-angle annular dark-field scanning transmission electron microscopy (HAADF-STEM) images were taken at 300 kV using FEI TitanCubed 300 kV Super Twin.

Spatially resolved CL studies were carried out at 10 K using an Attolight CL-scanning electron microscope (SEM) Alalin Chronos 4027 system with an acceleration voltage of 6 kV.[14] Time-resolved CL (TRCL) was performed using the same Attolight CL-SEM microscope, where the pulsed excitation was achieved using 1 ps electron pulses at a repetition rate of 80 MHz. A Jobin-Yvon (iHR320) spectrometer with a Synapse CCD camera and a Hamamatsu streak camera synchronized with the electron pulses were used as detectors. The nominal spatial and temporal resolutions of the CL system are 50 nm and 10 ps, respectively.

The surface morphology of the sample is shown in the AFM image in Fig. 1(a). Step bunches aligned along [11–20] are observed as a result of the macroscopic 2° miscut of the bulk *m*-plane substrate, but the surface in between the step bunches is flat and smooth. The typical step-height is ~30 nm. A cross-sectional HAADF-STEM image taken from a surface step shown in Fig. 1(b) reveals that the QW and barrier widths are uniform along the planar *m*-plane regions. In addition to the expected *m*-plane non-polar QWs, semi-polar QWs form at the step bunches close to {3-30-2} plane.[13] The average QW and barrier thicknesses along these semi-polar facets were measured to be 3.4 ± 0.4 nm and 6.9 ± 0.4 nm, respectively. An increase in indium content of 1.5 times on a typical semi-polar facet QW has been found and a more detailed microstructural analysis of the MQW structure and the surface steps can be found elsewhere.[13] Previously we reported low temperature (10 K) photoluminescence (PL) spectroscopy of the same sample, the spectrum was distinctly asymmetric with a pronounced low energy tail in the spectral region around 2.69 eV.[12] Based on correlated TEM and PL measurements, we attributed the low energy tail to recombination from the semi-polar QWs on the step bunches.[12,13]

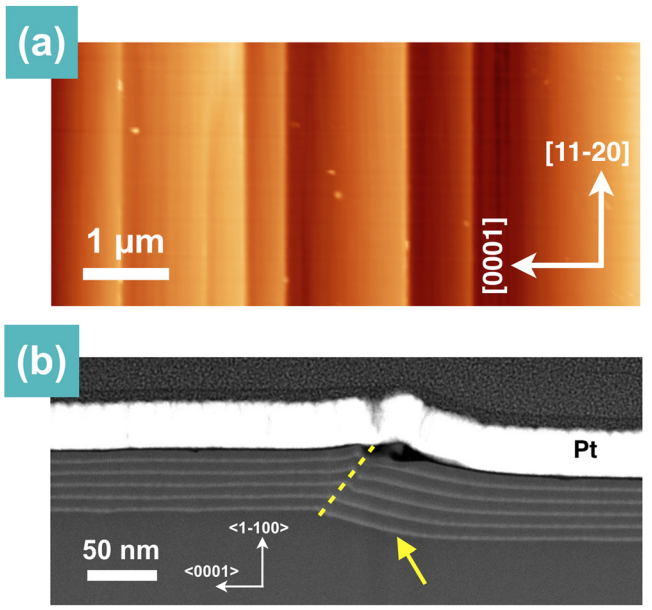

FIG. 1. (a) An AFM image of the InGaN/GaN 5QW sample grown on *m*-plane Ammono substrate with a miscut of 2° towards [000-1]. Z-scale is 60 nm. (b) Cross-sectional HAADF-STEM image reveals the formation of semi-polar QWs at the step in addition to the *m*-plane QWs. The yellow arrow indicates the position of a step bunch edge.

In order to investigate the optical properties further, spatially resolved SEM-CL measurements were first performed in continuous wave (CW) mode at 10 K. Fig. 2(a) shows the integrated CL spectrum over the entire scan area of 2.5 μm × 2.5 μm (Fig. 2(b)), which reveals a broad QW emission spectrum with a low energy tail. Spatially resolved CL spectra taken from the *m*-plane surface and a step edge are shown in Fig. 2(c). A single broad emission centred at 2.92 eV is seen when sampling the *m*-plane surface, while a strong emission at 2.69 eV and a weak emission at 2.89 eV are both present when sampling on the step edge. The monochromatic CL images show that the light from the planar *m*-plane surface is dominated by recombination from the *m*-plane InGaN QWs at 2.92 eV (Fig. 2(d)), and the light that is from the step edges is mainly due to the emission which peaks at 2.69 eV (Fig. 2(f)). The presence of the higher energy feature in Fig. 2(c) taken on the step is attributed to the effects of the finite electron beam spreading in the sample so that, to a degree, the *m*-plane QWs are also excited. Also the difference in the energies between the peak at 2.92 eV and 2.89 eV is attributed to the fact that, as can be seen in Fig. 1(b), on the right-hand side of the step, the transition from the semi-polar facet to the *m*-plane QWs is gradual, and this perturbs the QW emission energy. This is clearly evident in the CL image taken at 2.89 eV as shown in Fig. 2(e), where another bright band emission occurs adjacent to the step edge position. We note that the emission feature at ~2.89 eV appears unevenly distributed along the step bunch, which could be attributed to local inhomogeneous indium incorporation during the gradual transition from the semi-polar facet QWs into *m*-plane QWs. Therefore, by combining the CL, and TEM data, we show unequivocally that the low energy emission features originate from the step bunches where InGaN MQWs form

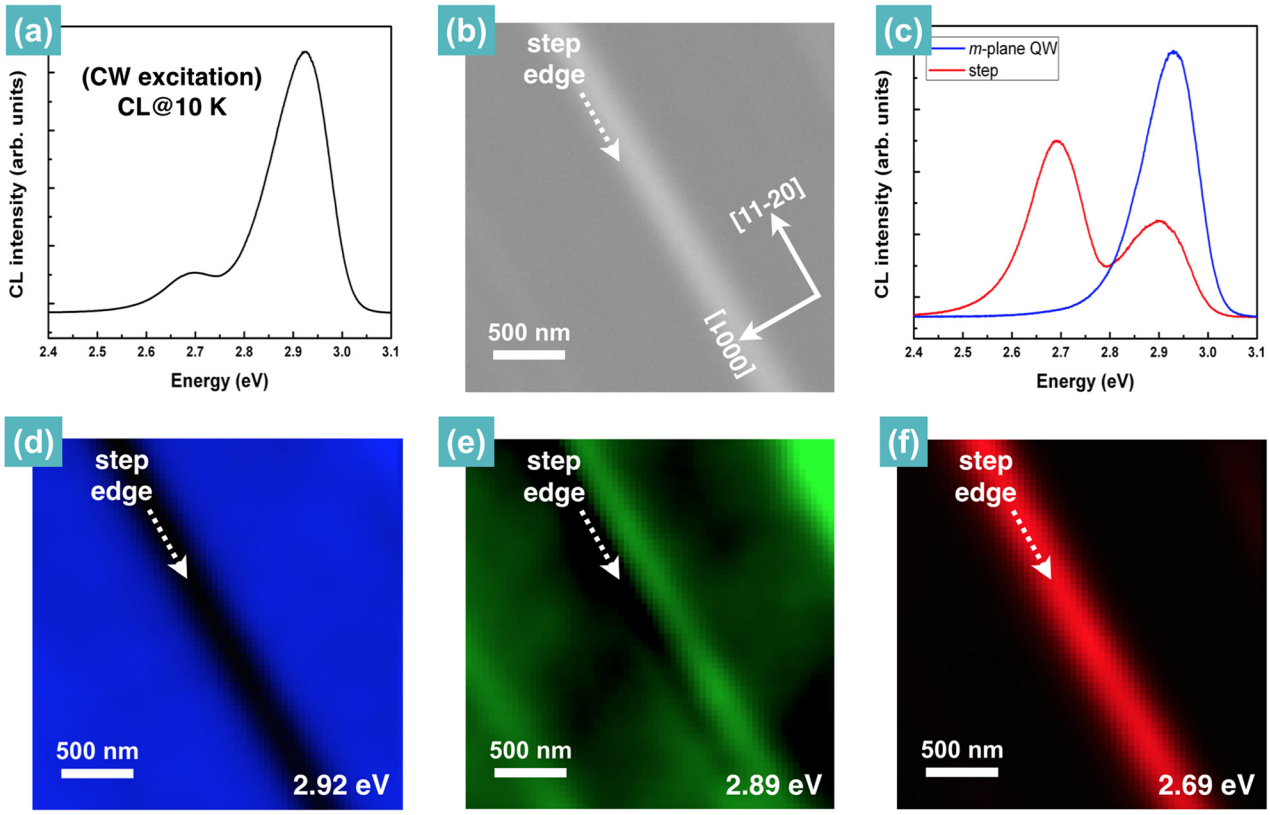

FIG. 2. SEM-CL data taken under CW excitation at 10 K. (a) Integrated CL spectrum over the entire scan area (2.5 μm × 2.5 μm) reveals a broad QW emission peak and a low energy tail. (b) SEM image of the corresponding area. (c) Spatially resolved CL spectra taken from the *m*-plane surface (blue line) and a step (red line). Monochromatic CL images taken at (d) 2.92 eV, (e) 2.89 eV, and (f) 2.69 eV.

on the semi-polar facets.[13] By calculating the emission wavelength using a $\mathbf{k}\cdot\mathbf{p}$ perturbation approach,[15,16] we can show that the large red-shift on the semi-polar facet QW can be mainly attributed to the significant increase in indium content and partly due to a change in the QW thickness. The internal electric fields are not the main factor, and the change of growth orientation, from *m*-plane to semi-polar (3-30-2) plane, only results in a negligible red-shift. (For calculated emission wavelengths with different indium contents and QW widths on different orientations, see supplementary material).

To investigate further the nature of the low energy emission from the semi-polar facet at a step edge, TRCL measurements were performed. After switching to pulsed excitation mode, similar time integrated spectra to the case of CW excitation were observed when exciting the sample away from the step edges and on a step edge as shown in Fig. 3(a). Consistent with the CL data obtained under CW excitation, the *m*-plane surface exhibits a single emission peak at 2.92 eV. On the step-bunch, a strong peak at 2.69 eV dominates and a small peak is also seen at ∼2.89 eV. The monochromatic CL images taken in pulsed mode shown in Figs. 3(b) and 3(c) again confirm that the planar *m*-plane surface is predominantly emitting at 2.92 eV, while the step emits at a lower energy around 2.69 eV.

TRCL measurements were performed by taking spatially resolved maps using the streak camera across a step bunch. The areas probed are illustrated by Fig. 4(a), which are superpositions of the CL intensity map taken at 2.92 eV (in blue) and the CL intensity map at 2.69 eV (in red). For areas outside a step bunch (points A and C), the CL transients (Figs. 4(e) and 4(g)) can be described over a significant range of the decay by a single time constant = 350 ps at a detection energy of 2.92 eV, this decay constant is similar to that recorded in the PL measurements reported elsewhere.[12] We note that there is a small red-shift (∼10 meV) for the 2.92 eV emission peak between points A and C (Figs. 4(b) and 4(d)), which can be attributed to local indium inhomogeneities. At the onset of the decay, the CL intensity decays more slowly than at later times forming almost a plateau-like region. We tentatively explain this behaviour by noting that the recombination process in *m*-plane non-polar QWs has been attributed to localised excitons. The localisation involves trapping of holes at regions of the InGaN QW where the distribution of In atoms is high on an atomic scale. Thus the holes can be thought of as being confined in a quantum dot. Thus if the hole ground states are saturated, state blocking effects can occur leading to a plateau region at the beginning of the decay similar to that which has been observed in InAs quantum dots.[17] We note that excitation dependent TRCL experiments might be used in the future to help demonstrate that the plateau at the early stage of the decay is related to localised states.

However, when the excitation spot lies mainly on the step bunch (point B) we have two emission bands. The streak image (Fig. 4(c)) from the main emission at 2.69 eV reveals a slowly decaying emission with time constant, 489 ps. This emission at 2.69 eV has been assigned to recombination involving semi-polar QWs on the step bunches. As semi-polar QWs are affected by an internal electric field along the

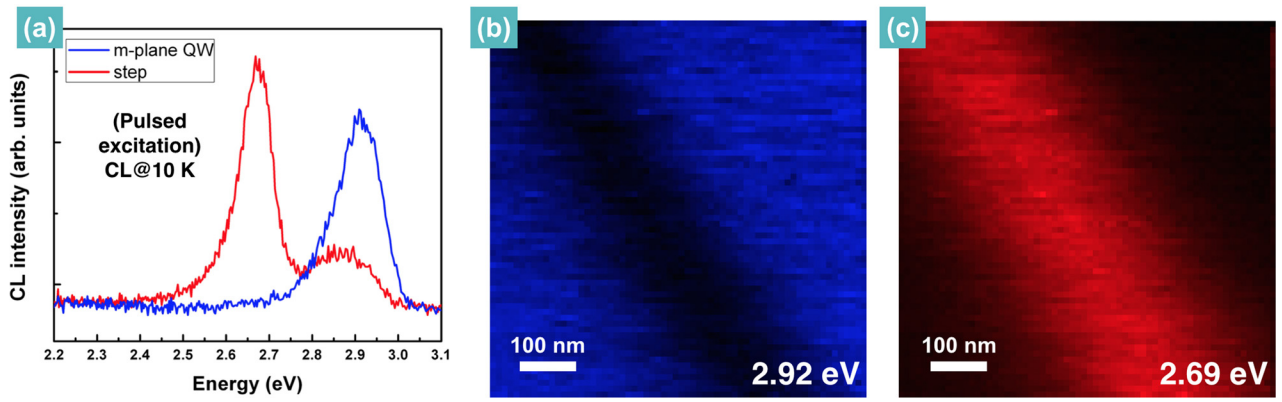

FIG. 3. (a) CL spectra taken under pulsed excitation at 10 K from the *m*-plane surface (blue line) and a step (red line). Spatially resolved monochromatic CL images taken at (b) 2.92 eV and (c) 2.69 eV.

[0001] direction, the resultant reduction in the electron-hole wavefunction overlap would also lead to reduced radiative recombination rates,[18,19] which is in agreement with the observation of a slow-decaying low energy emission feature. We have calculated the internal electric field in the QWs according to Refs. 20 and 21. The electric field would increase with indium content, and the effect is dependent on the angle from the non-polar orientation (For the calculated electric field with different indium content and QW widths on different orientations, see supplementary material). For an indium content of 31.5% and 3.4 nm InGaN well/ 6.9 nm GaN barrier,[13] the internal electric field for *c*-plane is found to be 3.8 MV/cm, 0 MV/cm for *m*-plane, and 0.42 MV/cm for semi-polar (3-30-2) plane. Compared to the *m*-plane case, the semi-polar (3-30-2) has a ~3% lower electron-hole wavefunction overlap integral if we do not consider the different indium contents and barrier thicknesses between the two facets. Taking into account the observed changes in the

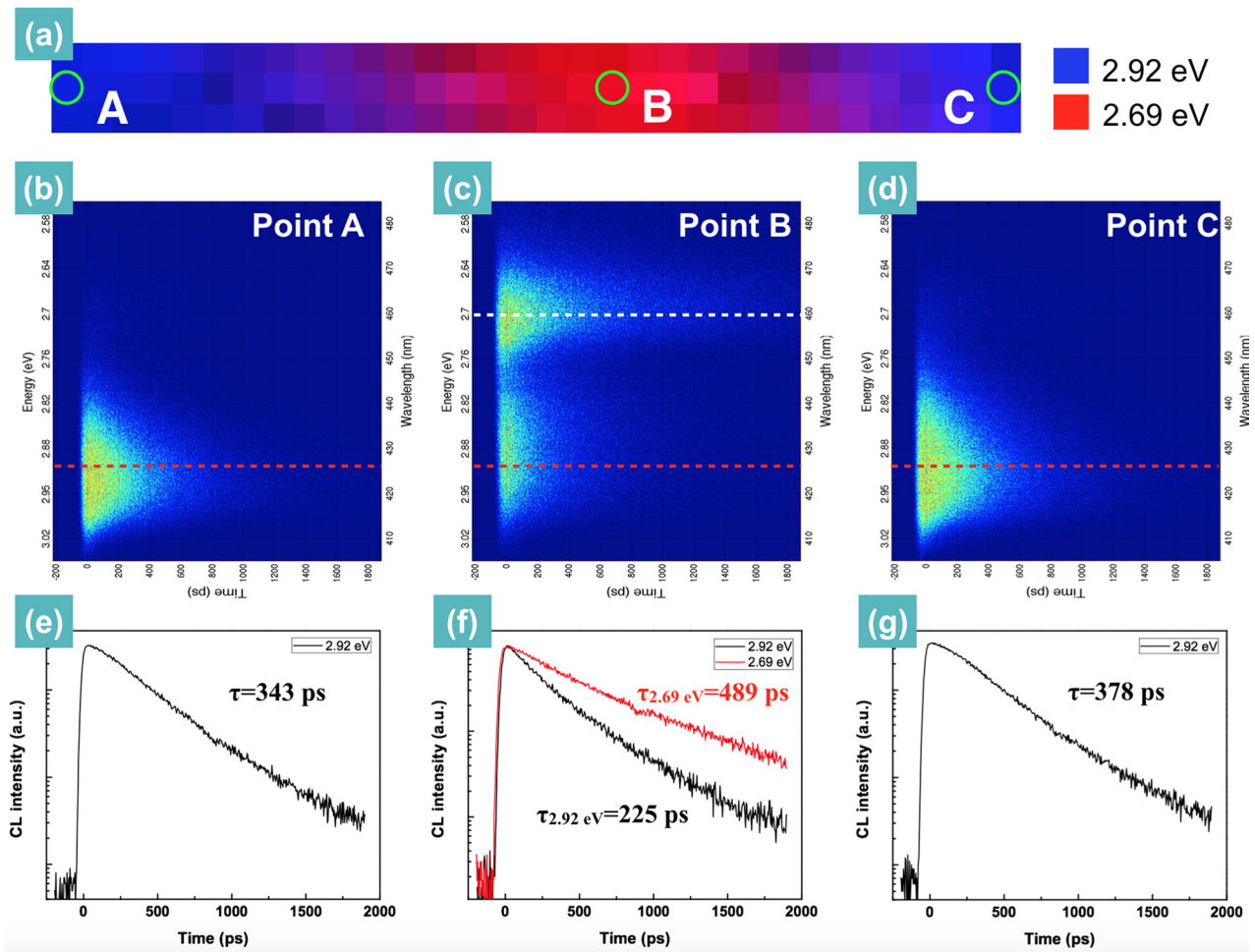

FIG. 4. (a) Overlaid monochromatic CL images taken at 2.92 eV and 2.69 eV illustrating the areas where streak camera maps were acquired by exciting and scanning along different positions of a surface step with a step/pixel size of 20 nm. (b)–(d) Streak camera images taken at different positions (A–C) across the step. CL decay spectra integrated over (e) 2.92 eV at point A, (f) 2.92 eV and 2.69 eV at point B, and (g) 2.92 eV at point C.

structural parameters, the reduction in overlap integral is ~6%. This is expected to lead to a reduction in oscillator strength and an increase in the radiative lifetime (For the calculated electron-hole wavefunction overlap integrals with different indium content and QW widths on different orientations, see supplementary material). In addition, we note that the changes in the In content in the semi-polar facet QWs could affect the lifetime also via changes to the localization environment. Furthermore, we note that the slow-decaying component has been measured with a lifetime longer than 1 ns by time-resolved photoluminescence.[12] This can be explained by the fact that the current TRCL system works at a repetition rate of 80 MHz and the maximal time span of the streak camera is currently limited at 2.1 ns.

As noted, not only do we observe emission from the semi-polar wells, we also observe emission at 2.89 eV from the non-polar wells close to the step bunches, which was attributed to inhomogeneous indium distribution during the gradual transition from semi-polar facet QWs into *m*-plane QWs close to the step bunch. The decay of this emission band is somewhat different from that when the electron beam is focused solely on the non-polar QWs (points A and C). Firstly we note the absence of the plateau region which we speculated was due to saturation of the localised quantum dot ground states. In these decay curves where the beam is focused primarily on the step bunches, the excitation density of the non-polar wells is much weaker and insufficient to saturate the ground states. We also note that the decay of the emission of QW emission energy (2.89 eV) at point B (on step) is faster with a time constant = 225 ps than that at points A and C where the time constant $\tau = \sim 350$ ps. There are two possible causes for this behaviour. The first is that the carriers in the non-polar wells can tunnel from the localised states into the semi-polar wells thus providing a faster non-radiative route which reduces the measured CL decay time from the non-polar wells close to the step bunches. An alternative explanation is that the decrease in decay time of the emission from the non-polar wells is due to non-radiative recombination associated with defects that form at the step bunches. TEM of the step bunches has revealed the formation of stacking faults in the step bunch region.[13]

In conclusion, we have reported spatially- and time-resolved CL measurements on of InGaN/GaN MQWs grown on the *m*-plane GaN substrate. Two spectral features were observed depending on the precise location of the electron beam excitation. The higher energy feature involved recombination from the *m*-plane QWs whereas the low energy emission feature was shown to arise from the recombination from semi-polar QWs across the step bunches produced by the miscut of the GaN substrate. This assignment was confirmed by the different time scales of the recombination; the recombination from the *m*-plane wells was faster than that from the semi-polar wells due to the absence of an electric field across the QWs. Although, it should be noted that the recombination dynamics of the *m*-plane QWs located close to the step bunches was perturbed either by carriers transferring to the semi-polar wells or recombining non radiatively at defects associated with the step bunches.

See supplementary material for the calculated electric field, emission wavelengths, and electron-hole wavefunction overlap integrals with different indium content and QW widths on different orientations.

This work has been funded by the EPSRC (Grant Nos. EP/J003603/1, EP/J001627/1, and EP/M011682/1) and in part by the European Research Council under the European Community's Seventh Framework Programme (FP7/2007-2013)/ERC Grants Agreement No. 279361 (MACONS).

Datasets for the figures in this paper can be found at https://doi.org/10.17863/CAM.6452.

[1]C. H. Chiu, S. Y. Kuo, M. H. Lo, C. C. Ke, T. C. Wang, Y. T. Lee, H. C. Kuo, T. C. Lu, and S. C. Wang, J. Appl. Phys. **105**, 063105 (2009).
[2]S. Marcinkevičius, K. M. Kelchner, L. Y. Kuritzky, S. Nakamura, S. P. DenBaars, and J. S. Speck, Appl. Phys. Lett. **103**, 111107 (2013).
[3]A. Chakraborty, B. A. Haskell, S. Keller, J. S. Speck, S. P. Denbaars, S. Nakamura, and U. K. Mishra, Jpn. J. Appl. Phys., Part 1 **44**, L173 (2005).
[4]E. Matioli, S. Brinkley, K. M. Kelchner, Y.-L. Hu, S. Nakamura, S. DenBaars, J. S. Speck, and C. Weisbuch, Light: Sci. Appl. **1**, e22 (2012).
[5]H. Masui, H. Yamada, K. Iso, S. Nakamura, and S. P. DenBaars, J. Phys. D: Appl. Phys. **41**, 225104 (2008).
[6]S. F. Chichibu, M. Kagaya, P. Corfdir, J.-D. Ganière, B. Deveaud-Plédran, N. Grandjean, S. Kubo, and K. Fujito, Semicond. Sci. Technol. **27**, 024008 (2012).
[7]S. Marcinkevičius, K. M. Kelchner, S. Nakamura, S. P. DenBaars, and J. S. Speck, Appl. Phys. Lett. **102**, 101102 (2013).
[8]S. Schulz, D. P. Tanner, E. P. O'Reilly, M. A. Caro, T. L. Martin, P. A. J. Bagot, M. P. Moody, F. Tang, J. T. Griffiths, F. Oehler, M. J. Kappers, R. A. Oliver, C. J. Humphreys, D. Sutherland, M. J. Davies, and P. Dawson, Phys. Rev. B **92**, 235419 (2015).
[9]K. Fujito, K. Kiyomi, T. Mochizuki, H. Oota, H. Namita, S. Nagao, and I. Fujimura, Phys. Status Solidi A **205**, 1056 (2008).
[10]R. Kucharski, M. Zając, R. Doradzińnski, M. Rudziński, R. Kudrawiec, and R. Dwiliński, Semicond. Sci. Technol. **27**, 024007 (2012).
[11]K. M. Kelchner, L. Y. Kuritzky, K. Fujito, S. Nakamura, S. P. DenBaars, and J. S. Speck, J. Cryst. Growth **382**, 80 (2013).
[12]D. Sutherland, T. Zhu, J. T. Griffiths, F. Tang, P. Dawson, D. Kundys, F. Oehler, M. J. Kappers, C. J. Humphreys, and R. A. Oliver, Phys. Status Solidi B **252**, 965 (2015).
[13]F. Tang, J. S. Barnard, T. Zhu, F. Oehler, M. J. Kappers, and R. A. Oliver, Appl. Phys. Lett. **107**, 082104 (2015).
[14]M. Shahmohammadi, G. Jacopin, X. Fu, J.-D. Ganière, D. Yu, and B. Deveaud, Appl. Phys. Lett. **107**, 141101 (2015).
[15]S. L. Chuang and C. S. Chang, Semicond. Sci. Technol. **12**, 252 (1997).
[16]Q. Yan, P. Rinke, A. Janotti, M. Scheffler, and C. G. Van de Walle, Phys. Rev. B **90**, 125118 (2014).
[17]P. D. Buckle, P. Dawson, S. A. Hall, X. Chen, M. J. Steer, D. J. Mowbray, M. S. Skolnick, and M. Hopkinson, J. Appl. Phys. **86**, 2555 (1999).
[18]M. Monavarian, D. Rosales, B. Gil, N. Izyumskaya, S. Das, Ü. Özgür, H. Morkoç, and V. Avrutin, Proc. SPIE **9748**, 974826 (2016).
[19]N. P. Hylton, P. Dawson, C. F. Johnston, M. J. Kappers, J. L. Hollander, C. McAleese, and C. J. Humphreys, Phys. Status Solidi C **6**, S727 (2009).
[20]A. E. Romanov, T. J. Baker, S. Nakamura, and J. S. Speck, J. Appl. Phys. **100**, 023522 (2006).
[21]T. Wernicke, L. Schade, C. Netzel, J. Rass, V. Hoffmann, S. Ploch, A. Knauer, M. Weyers, U. Schwarz, and M. Kneissl, Semicond. Sci. Technol. **27**, 024014 (2012).